SEATANI: hazards from seamounts in SouthEast Asia, Taiwan, and Andaman and Nicobar Islands (eastern India)

Andrea Verolino (andrea_verolino@hotmail.it)
Earth Observatory of Singapore https://orcid.org/0000-0002-9335-3993
Su Fen Wee
Nanyang Technological University
Susanna Jenkins
Nanyang Technological University https://orcid.org/0000-0002-7523-1423
Fidel Costa
Institut de Physique du Globe de Paris
Adam Switzer
Nanyang Technological University https://orcid.org/0000-0002-4352-7852

Article

Keywords:

Posted Date: September 18th, 2023

DOI: https://doi.org/10.21203/rs.3.rs-2950249/v2

Additional Declarations: Yes there is potential Competing Interest. In order to avoid any conflict of interest, we declare that co-author A.D. Switzer is a member of the editorial board for Communications Earth & Environment (Ocean and Cryosphere).

SEATANI: hazards from seamounts in SouthEast Asia, Taiwan, and Andaman and Nicobar Islands (eastern India)

Andrea Verolino[1], Su Fen Wee[2], Susanna F. Jenkins[1,2], Fidel Costa[1,2,3], Adam D. Switzer[1,2]

[1]Earth Observatory of Singapore, Nanyang Technological University, 50 Nanyang Ave, Singapore, 639798, Singapore
[2]Asian School of Environment, Nanyang Technological University, 50 Nanyang Ave, Singapore, 639798, Singapore
[3]Institut de Physique du Globe de Paris, Université Paris Cite, CNRS, 1 Rue Jussieu, Paris, 75005, France

Correspondence to: Andrea Verolino
Email: andrea.verolino@ntu.edu.sg

Abstract. Submarine volcanism makes up approximately 85% of volcanism taking place on Earth, and its eruptions can be particularly hazardous, with the potential to cause large-scale sector collapse of the volcanic edifice, tsunamis, and ash dispersal. Recent examples include the eruptions in Japan and in the Kingdom of Tonga in 2021 and 2022 respectively, but there has been little to no study of submarine volcanoes in Southeast Asia and its surroundings. Here we provide a compilation of 466 seamounts from the region, from different published sources, through the SEATANI dataset (Southeast Asia + Taiwan + Andaman & Nicobar Islands). We use this newly compiled dataset to assess on a regional basis the seamount hazard potential and exposure potential as a springboard for future more quantitative hazard studies for the region. The hazard potential was assessed through seamount morphological/structural analyses, to determine the seamount evolution stage and, grade of maturity. The exposure potential was evaluated through two different approaches: An areal analysis of the number of assets within a 100 km radius of each seamount; and the development of a hazard-weighted seamount density map to highlight potential areas of interest for future more-in-depth studies. Our results show that there are several potentially hazardous seamounts in this region, and Taiwan had the highest hazard and exposure potential, for all assets considered, while Philippines, Indonesia and Vietnam have relatively high exposure potential for submarine communication cables and ship traffic density. The results from this work serve as a first step for southeast Asian and neighbouring countries to become more resilient against and prepared for submarine volcanic eruptions in the region.

1 Introduction

Volcanic seamounts are submerged or mostly submerged volcanoes, and can be defined as "*any geographically isolated topographic feature on the seafloor taller than 100 m, including ones whose summit regions may temporarily emerge above sea level*" (Staudigel et al., 2010). The number of volcanic seamounts around the world is in the order of tens of thousands. A recent estimate suggests that there are ~35,000 seamounts >400-m in height (Gevorgian et al., 2023); however, limitations in detection suggest that this is a significant underestimate, especially in shallow continental shelf regions close to land masses (Kim and Wessel, 2011). Volcanic seamounts are generally detected through satellite-derived altimetry and gravimetry, however, these methods are limited by resolution (i.e. kilometric scale, not allowing for the detection of small seamounts), and noise in the gravimetry measurements in areas with thick sequences of sediments (e.g. within continental margins; Kim and Wessel, 2011). It is likely that there are many more seamounts globally than those we are aware of.

Traditionally, volcanic seamounts, particularly deep-sea ones, have been considered a negligible threat to society (Cas, 1992; Whelley et al., 2015), for several reasons. The first is that the majority of them lie completely underwater, hence are difficult to monitor compared to their subaerial counterparts; as a result, their eruption frequency and intensity cannot be properly assessed. A second reason is that they are often located far from major landmasses, hence not considered an imminent threat to populations. Thirdly, most of them have their summit in deep waters (> 3000 m b.s.l.), and this makes them hypothetically less hazardous than shallower volcanoes, because of the high hydrostatic pressure hindering explosivity. Another aspect is that since they are underwater, it is logistically and economically difficult to access them directly for sampling and detailed mapping. Finally, most ocean intraplate volcanoes, particularly those approaching subduction zones, are likely to be extinct and have not been active for millions of years (Staudigel and Clague, 2010), hence, have been not considered of interest for volcanic hazard. As a result, seamounts are vastly understudied around the world. In January 2022, the eruption of Hunga volcano in the SW Pacific (Kingdom of Tonga), demonstrated that erupting seamounts can have a large impact on people and their activities, even in a remote location such as the southwest Pacific Ocean. The eruption produced the highest volcanic plume ever recorded (~58 km) (Taha et al., 2022), unusually fast tsunamis that travelled across the Pacific Ocean for thousands of kilometres (Gusman et al., 2022), and damage of millions of USD across the entire region, with the Kingdom of Tonga being the most affected (damage equivalent to ~19% of the national GDP, and several casualties recorded) (The World Bank, 2022).

A few notable seamounts around the world have been studied in detail. Multibeam surveys have been conducted over these seamounts to obtain high resolution bathymetry (up to 1-m), and in very few cases were accompanied by sampling and/or video recording of the eruptions from Remotely Operated Vehicles (ROV's). Typically, these investigations occur after an impactful eruption. Examples include Havre volcano, in the Kermadec arc (north of New Zealand), which erupted in 2012 and produced what is considered one of the largest submarine silicic eruptions ever recorded (Carey et al., 2014; Murch et al., 2019a; Dürig et al., 2020); NW Rota-1 in the Mariana arc (Embley et al., 2006; Chadwick et al., 2008; Schnur et al., 2017), and West Mata in the Tonga arc (Clague et al., 2011; Dziak et al., 2015; Murch et al., 2022), which produced medium-intensity Strombolian explosions and lava flows (both eruptions were recorded); Fani Maoré volcano, offshore Mayotte island (NW of Madagascar), which was formed between 2018 and 2019, growing more than 800-m from the seafloor, and erupting both explosive and effusive products, despite being mostly basanitic in composition (Feuillet et al., 2021); Axial caldera, on the Juan de Fuca ridge (offshore of California, USA), which produced several effusive basaltic eruptions in recent years (last eruption in 2015), but also has evidence of past large explosive eruptions (Hammond, 1990; Caress et al., 2012; Clague et al., 2013), among others. All the above-mentioned submarine volcanoes were surveyed as part of large, well-funded, multidisciplinary projects that provided a wealth of data (bathymetry, rock geochemistry, tephra granulometry and componentry, etc.). It is logistically impossible to apply the same approaches to the thousands of seamounts worldwide, therefore, a regional approach is needed to characterise seamounts in a simple and efficient manner that allows for a broad focus on lesser-known areas potentially at risk.

Past studies on volcanic seamounts have been conducted globally and at times included classifications based on their morphology or growth stage (Schmidt et al., 2000; Wessel, 2007; Staudigel and Clague, 2010; Kim and Wessel, 2011; Gevorgian et al., 2023). Some authors found direct relationships between seamount morphometric parameters (e.g. basal width and height) and linked them to the tectonic setting (Schmidt et al., 2000; Gevorgian et al., 2023). These classifications, however, have never been used for assessing hazard potential or exposure on a regional scale.

In the particular case of Southeast Asia (SEA), there has been some effort in assessing hazards from what we define here as volcanic seamounts; examples include Krakatau and Banua Wuhu, Indonesia, and Didicas, Philippines (Hamzah et al., 2000; Paris et al., 2014; Mutaqin et al., 2019; Hidayat et al., 2020; Zorn et al., 2022; NCEI/WDS, n.d.), however, these studies focused on volcanic islands, and there is little or no consideration for the hazard potential from fully submerged volcanoes in the region.

Our newly compiled dataset includes 466 seamounts from different sources (Fig. 1, Table S1 – Supplementary information) and enclosed within three (Indonesia, Philippines and Vietnam) of the nine Exclusive Economic Zones (EEZs) of Southeast Asia (Brunei, Burma, Cambodia, Indonesia, Malaysia , Philippines, Singapore, Thailand and Vietnam) and the neighbouring countries Taiwan and eastern India (Andaman and Nicobar Islands), and has been named SEATANI (**SEA** + **T**aiwan + **A**ndaman & **N**icobar **I**slands). This dataset includes both fully submerged volcanoes and some small volcanic islands, whose submerged portion makes up the majority of the edifice.

We chose this region for several reasons: (i) The whole area is very volcanologically active, but little is known about its underwater features; (ii) There are millions of people living along the coasts of countries in the region; (iii) There are infrastructure worth billions of dollars on the seafloor of the target area (e.g. submarine telecommunication cables) (Wang et al., 2019); And (iv) density of ship traffic in the region is rather high. Based on this, we 1) characterise the seamount morphology and evolution stage and link them to the *hazard potential* for seamounts in the region; and 2) highlight areas of high *exposure potential*, in order to motivate and focus future studies. To accomplish the first goal of characterising seamounts and assess their hazard potential, we conduct qualitative (seamount type: caldera, guyot, simple cone, composite cone) and quantitative morphological analysis (height, summit water depth) by using open-access bathymetry datasets (e.g. Gebco 2021; NOAA DEM Global Mosaic; NOAA Multibeam Bathymetry Mosaic). Additionally, in support of goal 1, we conduct a more qualitative analysis based on higher resolution bathymetry (Multibeam data from NOAA – 90m/pixel), where we highlight key seamount features (e.g. submarine landslides, explosive craters, new seamounts) that otherwise would not be detected from Gebco or the NOAA DEM Global mosaic dataset. Despite the multibeam data having limited regional coverage (< 10%), they reveal significant seafloor morphologies that can motivate future quantitative hazard assessments for the region, e.g. numerical hazard modelling. The second goal of highlighting areas of high exposure potential is achieved through two types of analysis, a quantitative one, where the number of assets and activities (population, submarine fibre-optic cables, and ship traffic density) within 100 km of volcanic seamounts is counted; and a semi-quantitative one, where the hazard potential of each seamount is used to weight the potential areal hazard extent for the entire region of interest. We acknowledge that our work comes with some limitation, in particular, hazard and exposure potential are not quantified based on geological, geochemical, tectonic setting, age, and frequency/magnitude information, which are indeed needed for more quantitative studies (a focused discussion is provided later in the text to address these points). However, our intent with this work is to provide the basic but fundamental elements for future more quantitative studies.

2 Methods

2.1 Compilation of SEATANI

Following the seamount definition from Staudigel et al. (2010), here only used for volcanic seamounts, we pre-compiled a list of seamounts for the region of interest by using three different types of sources: 1) The GVP database (Global Volcanism Program 2013), where we include seamounts that have erupted from the Pleistocene (n= 42); 2) The seamount dataset Gevorgian et al. (2023) (n= 405), which is an updated version of the dataset from Kim and Wessel (2011), where they used statistical methods to differentiate volcanic from non-volcanic seamounts; and 3) Seamounts from individual studies around the southeast Asian region found in literature (n= 35) (Li et al., 2013; Fan et al., 2017), which have been detected through geophysical methods (i.e. interpretation of seismic profiles), for a total of 482 entries for the region considered. The definition proposed by Staudigel and colleagues, however, does not provide specific directions on islands (at what extent a volcanic island is still considered a seamount), therefore, in order to guarantee reproducibility, we did not include islands whose emerged volume was > 30% of the total seamount volume, and/or their maximum elevation was > 1000 m a.s.l. (more details on this methodology are provided in the supplementary information). Following this criterion, none of the seamounts from the Gevorgian et al. dataset or from the literature studies were removed, however, 16 GVP volcanoes were excluded (Table S2, Supplementary information), bringing the total to 466 volcanic seamounts. Despite the choice of 30% and 1000 m a.s.l. was somewhat arbitrary, it allows comparisons across studies and is in line with our focus here, which is primarily on submarine volcanoes.

2.2 Bathymetry and exposure datasets

For the bathymetry, we used different datasets of different resolution based on each specific purpose, namely *Gebco 2021*, *DEM global mosaic* (from NOAA/NCEI), and *Multibeam Bathymetry Mosaic* (from NOAA/NCEI). Gebco 2021, a gridded bathymetric dataset with interval grid of 15 arc-second (450-m/pixel), was used for the quantitative morphological classification (seamount growth stages) and exposure potential analyses (quantitative and semi-quantitative). Despite the relatively low/medium resolution, it has global coverage with bathymetry data deriving from different acquisition methods (Fig. S1, supplementary material), and was clipped for the region of interest (North: 36.5°, South: -14.3°, West: 82.0°, East: 145.6°). The DEM global mosaic is a colour shaded relief raster file that was exclusively used for the qualitative morphological classification (seamount morphotypes); it is a seamless bathymetry/topography mosaic that combines DEMs from several sources (e.g. direct and indirect measurements from ships and satellites) and different resolutions (450-m/pixel or better), with the higher-resolution DEMs displayed on top of the lower resolution ones (where both available). Since DEMs of different resolution cannot be extrapolated from this file, but must be downloaded individually, we used the mosaic format for efficiency and for visualization purposes only. The file was clipped with the same extent as Gebco 2021, for consistency. The Multibeam Bathymetry Mosaic is the dataset with the highest resolution among the datasets used here (90-m/pixel); it is a gridded colour shaded relief, deriving from multibeam survey data collected over the years (from ~1980 to present). This dataset has a coverage lower than 10% for the region of interest, therefore was only used for qualitative image analyses, both for the morphological classification (in combination with the

DEM Global mosaic) and for the characterization of bathymetric features (see discussion) at some of the locations enclosed within our study area (where there was data coverage).

To assess the exposure potential, we used different open-access datasets for population, submarine communication cables and ship traffic density. We chose these assets for three reasons: (i) Data were available for quantitative analyses on GIS environment on a regional scale; (ii) We considered them as the assets potentially more exposed to multiple hazards from a submarine volcanic eruption in a regional perspective (e.g. air traffic exposure was not quantified here because potentially only exposed to development of a tephra column); And (iii) such exposure assessment from submarine volcanic eruptions has not been done before, particularly for submarine communication cables and ship traffic density, which instead have shown to be vulnerable elements to natural hazards (Ohno et al., 2022; Speidel, 2022). For population estimates, we used LandScan (Sims et al., 2022), which has a spatial resolution of around 1 km (30 arc-seconds) and has been widely used in previous volcanic hazard assessments (Reyes-Hardy et al., 2021; Jenkins et al., 2022; Verolino et al., 2022a). For the submarine cables we used data from *TeleGeography* (last update in 2017); while for the ship traffic density we utilised data from *The World Bank Group*, which reports hourly Automatic Identification Systems (AIS) positions, recorded between January 2015 and February 2021, at a spatial resolution of 500-m/pixel. This dataset included separate files for commercial, leisure, passenger, oil and gas, and fishing vessels respectively, however, we used the combined file, assuming no distinction across vessel types.

2.3 Volcanic seamounts classification

Volcanic seamounts in the region of interest were classified through two different approaches: 1) Qualitative, based on seamount shape (i.e. caldera, guyot, simple cone, composite edifice; Fig. 2 and Table 2); and 2) Quantitative, based on the seamount height and depth that gives a stage of growth, as proposed by Staudigel and Clague (2010) (Stage 1 to 5: defined in Table 3). Both classifications were obtained from analyses conducted in GIS environment (Esri® ArcMap 10.7.1). For the qualitative classification, we overlaid the seamount locations over the bathymetry datasets, and conducted visual image analysis to establish morphotype (Table 2, Fig. 2), using the highest resolution available for that particular area (NOAA DEM Global Mosaic, 450-m resolution or better, or NOAA Multibeam data, 90-m resolution). This morphological assessment was conducted by authors A. Verolino and S.F. Wee, in order to verify consistency and reproducibility, being the classification partially subjective. For the quantitative method, here we applied the Staudigel and Clague (2010) classification (used here for the first time for hazard purposes) and obtained the seamount maximum summit height and base water depth within a 30 x 30 km bounding box of the given seamount location (following Kim and Wessel, 2011). These were in turn used to assign a stage of growth. Staudigel and Clague (2010) also included Stage 6 seamounts (those approaching the trench of a subduction zone, or that already started being subducted), however, to maintain the growth stage classification in a state that is as quantitative as possible, we included them within the low hazard potential i.e. Stage 1, 2 or 5 seamounts (i.e. deep-water or extinct seamounts). We did this depending on their height and water depth though we know that the Staudigel and Clague (2010) classification, is not specific on how close to the subduction trench a seamount must be to be considered stage 6, leaving some subjectivity in the classification). We used both qualitative and quantitative classification approaches in parallel in order to obtain different types of information (morphological and growth stage); however, for exposure calculation we refer only to the quantitative approach (i.e. growth stage).

2.4 Exposure analysis

We conducted two types of exposure potential assessments: 1) A quantitative analysis of population, submarine communication cables and ship traffic density within 100 km from each seamount; and 2) A semi-quantitative assessment, through a hazard-weighted seamount density map, to assess what countries are more likely to be threatened by a seamount within the study region.

For the first type of assessment, we chose concentric 100 km radii to include exposure potential of the above-mentioned assets with the approximation that this would include the more damaging processes from most volcanic hazards (e.g. tephra fallout, PDCs, sector collapses). This choice is in line with previous regional volcanic threat studies (Small and Naumann, 2001; Brown et al., 2015), however, we acknowledge that using concentric radii is an oversimplification of volcanic hazard extents (Jenkins et al., 2022).

The semi-quantitative assessment considered the concentration of seamounts, weighted by their hazard rank (Table 1), and highlights regions of higher hazard potential. We created a weighted seamount density map (Kernel Density Estimation, KDE), based on the seamount stage of growth, with the assumption that more heavily weighted seamounts have a greater hazard potential. The KDE was performed on Esri® ArcMap 10.7.1, which assigns a default bandwidth in function of the input dataset (~626 km in this case), and proven to be reliable in previous exposure studies (Verolino et al., 2022a). The choice of weight assigned to each growth stage (Table 1) was based on the Global Historical Tsunami Database (NCEI/WDS), where out of 164 historical volcanic tsunamis (from 1610 BC to present), 115 were from volcanic seamounts; of these, 78% (n= 90) were from stage 4, 20% (n= 23) from stage 3, and nearly 2% (n= 2) from stage 1, 2, 3 or 5 seamounts (depth of seamount unknown). In order to compensate the paucity of historical information/data from stages 3, 2, 1 and 5 (shallow or deep), compared to stage 4 seamounts (partially emerged), and to include volcanic hazards as well, we arbitrarily adjusted these percentages to 60% and 35% for stage 4 and stage 3 respectively, and the rest was distributed through stage 1, 2 and 5 seamounts (Table 1). Exposure potential was then assessed based on the extent of high-density area (higher exposure potential: > 2.9×10^{-6} seamounts/km^2) obtained from the KDE.

Table 1. Seamount hazard ranking based on the Global Historical Tsunami Database (NCEI/WDS) and growth stage from Staudigel and Clague (2010).

Seamount hazard ranking	Seamount growth stage	Historical volcanic tsunami occurrence (%)	Hazard weight
1	4	78	0.6
2	3	20	0.35
3	2		0.03
4	1	2	0.01
5	5		0.01

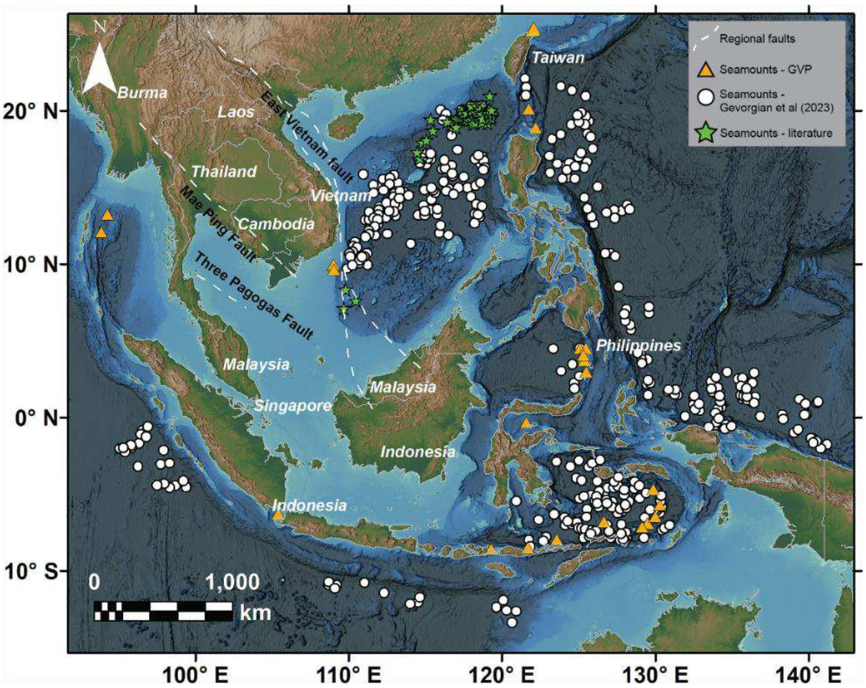

Figure 1. Map of the study area with seamounts locations and major regional faults. Basemap is from NOAA (DEM Global Mosaic).

3 Linking seamounts morphology and evolution stage with their potential hazards

3.1 Seamount morphotype

Seamount morphology provides hints about the seamount eruptive history. An important consideration is that once seamounts are completely submerged, they do not experience major erosion, retaining most of their original morphological constructive features, unless new eruptions and/or disruptive events such as landslides take place. Therefore, classifying seamounts based on their large-scale morphological features overcomes the resolution issue that we generally have at smaller scales. Below in Table 2 (examples shown in Fig. 2), we provide general guidelines used here for the classification of seamount morphotypes. A background for each morphotype, with a link to their hazard potential and with relevant examples from the literature, is provided in the supplementary information file.

Table 2. Seamount morphotype descriptions.

Seamount morphotype	Description
Simple Cone	Regular-shaped and conical pointy volcanic edifice with only one vent
Composite edifice	Irregularly shaped volcanic edifice with one or more vents. This morphotype also includes ridges and flank ephemeral cones (e.g. subaqueous portion of a volcanic island)
Caldera	Volcanic edifice with prominent central depression with diameter ~ 4-8 km
Guyot	Flat-topped volcanic edifice with relatively steep flanks

3.2 Seamount growth stage

Staudigel and Clague (2010) classified seamounts based on their growth stage (Stage 1 to 5), here we use the same approach to first assign a growth stage to the SEATANI seamounts, and then link the growth stage to a given potential hazard(s) that may be common for that particular growth stage. In Table 3 we report the main characteristics for each growth stage (from Staudigel and Clague, 2010), and associated potential hazards (Murch et al., 2019a; Paris et al., 2014; Clague et al., 1990; Harders et al., 2014; Verolino et al., 2018, 2019, 2022b; Jutzeler et al., 2014; Deardorff et al., 2011; Omira et al., 2016; Newland et al., 2022). A more comprehensive analysis of seamount growth stages and their potential hazards is provided in the supplementary information file.

Table 3. Seamount growth stage and associated potential hazards. Adapted from Staudigel and Clague (2010).

Seamount growth stage	**Description** (from Staudigel and Clague, 2010))	**Potential hazards** (see references in the text)
1	● Seamounts 100-1000 m high and > 700 m b.s.l. ● > 80% lavas and < 20% pyroclastic deposits	● Lava flows ● Obstacles for navigation (submarines)
2	● Seamounts > 1000 m high and > 700 m b.s.l. ● > 80% lavas and < 20% pyroclastic deposits ● Developed shallow magma plumbing system (especially the larger ones), potentially leading to flank instability	● Lava flows ● Subaqueous eruption-fed density currents ● Subaqueous eruption column ● Pumice rafts ● Large gas bubbles ● Sector collapse ● Tsunamis ● Obstacles for navigation (submarines)
3	● Seamounts < 700 m b.s.l. ● > 60% pyroclastic deposits ● +/- Developed shallow plumbing system (depending on seamount size) ● Higher flank instability due to abundance of pyroclastic material making up the seamount	● Lava flows ● Subaqueous eruption-fed density currents ● Subaerial PDCs ● Subaqueous and subaerial eruption column ● Pumice rafts ● Sector collapse ● Tsunamis ● Obstacles for navigation (submarines)
4	● Emerged seamounts (> 70 vol% submerged) ● > 60% pyroclastic deposits ● +/- Developed shallow plumbing system (depending on seamount size) ● High flank instability due to abundance of pyroclastic material making up the seamount	● Lava flows ● Subaqueous eruption-fed density currents ● Subaerial PDCs ● Subaerial eruption column ● Sector collapse ● Tsunamis
5	● Flat-topped seamounts (guyots) ● Originally emerged seamounts drowned below sea level for erosion and subsidence, and cessation of volcanic activity	● Obstacles for navigation (submarines)

4 Results

4.1 Seamount morphology and growth stage

Seamounts in our study were classified based on their morphotype (simple cone, composite edifice, caldera, guyot; Fig. 2, Table 2) and growth stage (Stage 1 to stage 5; Table 3). Results for their abundance, distribution and exposure analyses are reported below (Figs. 3-6).

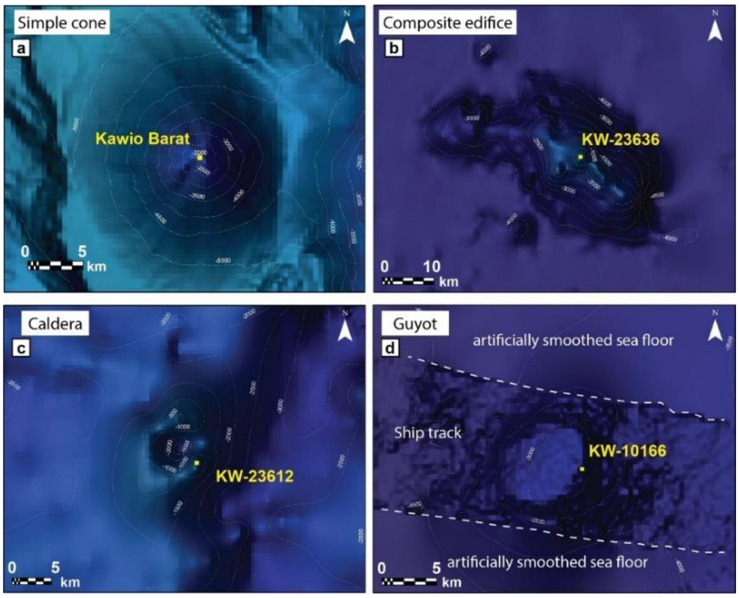

Figure 2. Seamount morphotype examples. Note how the seafloor appears smoothed away from ship track measurements due to low density of data points (d). The basemap shown here is from NOAA (DEM Global Mosaic).

Of the 466 seamounts in our catalogue, we were able to classify 295 (63%) of them into the four morphotypes; the remaining 171 (37%) seamounts were not classifiable due to low resolution bathymetry data and/or because they were too small. The seamounts are dominated by *composite* edifices (n= 255, 54.7%), followed by *simple cones* (n= 29, 6.2%), and guyots (n= 7, 1.5%). The morphotype least represented is calderas, with only 4 of them (0.9%). Water depths range from -5739 m b.s.l. (seamount KW-22106 of unknown morphotype; Lat: 13.81°, Lon: 125.58°) to 776 m a.s.l. (Paluweh, simple cone; Lat: -8.32°, Lon: 121.71°), with a *mode* of 2306 m b.s.l., *mean* -2106 m b.s.l., *median* -2221, and *skewness*= 0.02 (close to symmetric distribution) (Fig. 3c). Water depths within each morphotype category are relatively variable (Fig. 3d). Simple cones, composite edifices and calderas have a median of about 2000 m b.s.l., while guyots are mostly closer to sea level (median ~500 m b.s.l.), and unclassified seamounts cover the entire underwater range (~ 0-5700 m b.s.l.). Despite having a general broad range of water depths, all the classified seamounts are also represented at relatively shallow water depths (shallower than 1000 m b.s.l.), and this has important implications in terms of volcanic hazard (discussed in later sections). We found no particular geographic or tectonic setting distribution associated with each morphotype (Fig. 3a).

Results from the growth stage analysis (Fig. 3e) show that the majority of the seamounts in the study region are in their *stage 2* (n= 303), > 1000 m high and > 700 m b.s.l., followed by the shorter but still deep *stage 1* (n= 67), shallower *stage 3* (n= 58), and emerged *stage 4* (n= 31) seamounts. Only 7 seamounts represent *stage 5, flat-topped seamounts*. When comparing morphotype and growth stage distributions (Fig. 3f), simple cones and composite edifices are found in all growth stages, except for stage 5 (by definition), with composite edifices dominating across all stages. Calderas are only found within stage 2 (1%) and stage 3 (2%) seamounts, however, when a caldera complex has new cones formed within them or on their rims, we classified them as composite edifices (e.g. Krakatau, Indonesia). Undefined seamounts dominate stage 1, however, they decrease in percentage towards higher stages seamounts. In terms of geographic/tectonic setting, stage 1 and 2 seamounts dominate extensional and/or intraplate domains such as backarc basins (e.g. Banda Sea), and zones undergoing subduction (e.g. west of the Sumatra and Java trenches; east of the Philippines trench); while stage 3 and 4 seamounts are more common along volcanic arcs (e.g. Banda arc) and on the continental platform in proximity of regional faults (east of Vietnam; Fig. 1). An exception is represented by the South China Sea, an intraplate extensional setting, where the distribution of all grow stage seamounts is rather uniform.

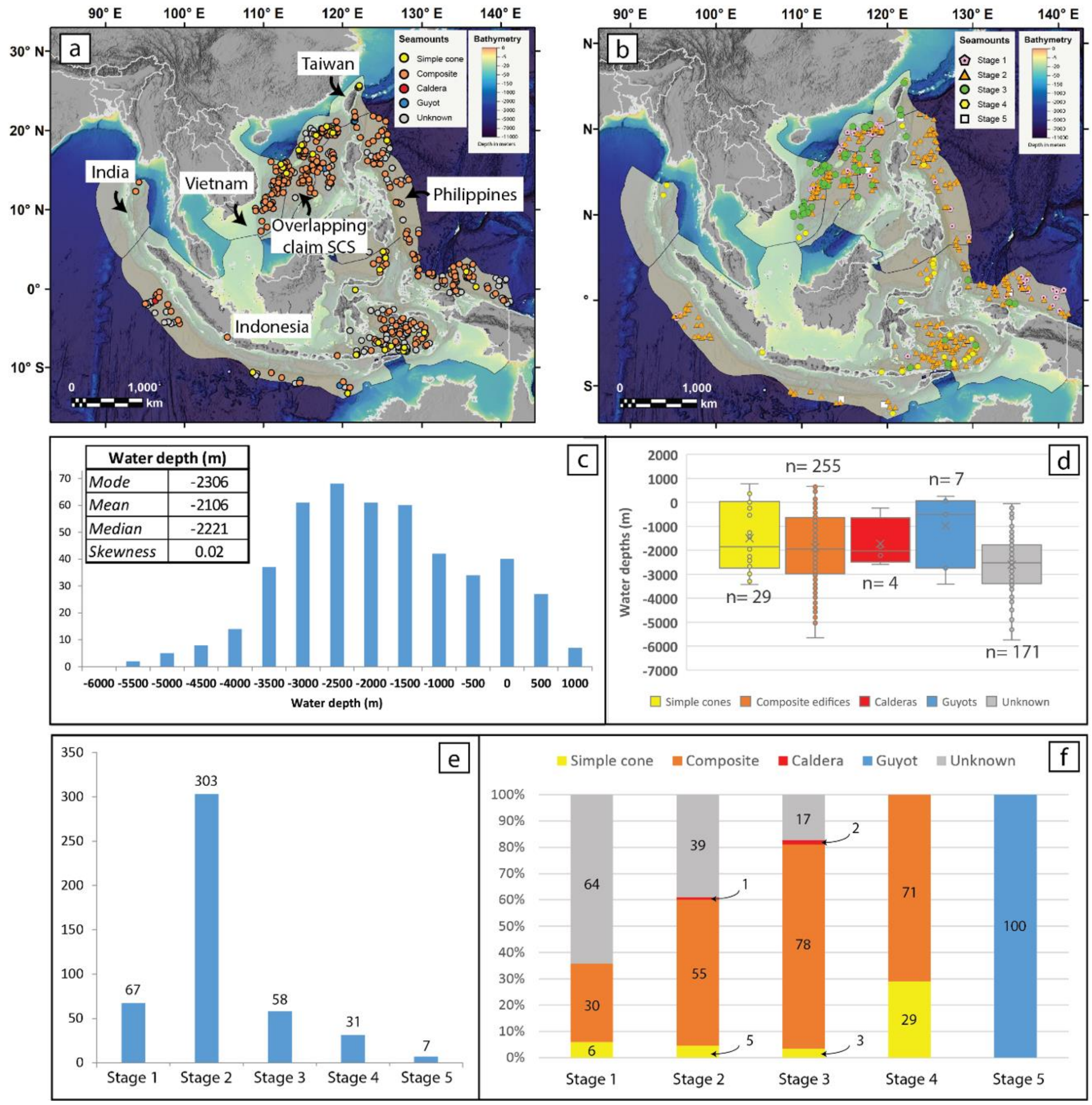

Figure 3. Results of seamount classifications. Seamounts distribution maps based on their morphotype (a) and growth stage (b) (basemap is from NOAA - DEM Global Mosaic). Distribution plots of water depths (c), and water depths vs morphotypes (d). Distribution of seamount growth stages (e), and normalised distribution (%) of seamount morphotypes within each growth stage (f).

4.2 Analysis of 'Exposure Potential'

4.2.1 Exposure Potential of assets around seamounts (quantitative)

In this section we assess the exposure potential for population, submarine communication cables and ship traffic within 100 km radius from each seamount (Figures 4 and 5; Fig. S2 and Table S1). We found that 1.3% of the volcanoes of our catalogue (n= 6) have more than 1M people living within 100 km from them, with Huapinghsu (about 40 km north of Taiwan) exposing about 9.6M people, and two nearby volcanoes (Mienhuayu and Pengchiahsu) having a similarly high level of exposure (8.2M and 6.8M people), with Taipei lying approximately 60 km away. Krakatau volcano, Indonesia, also ranks high, with nearly 8M people exposed (Fig. 4, Fig. S2), many in Jakarta, which lies ~140 km to the east. About 8% (n= 39) of the seamounts expose between 100k and 1M people, and these are mostly located within the EEZs of Taiwan, Philippines and Indonesia. There are also a significant number of seamounts (n= 319) with zero population exposure, mostly located in the central portion of the northern South China Sea, western Pacific Ocean, and eastern Indian Ocean, and some in the Banda Sea.

Exposure for submarine cables has been evaluated in terms of total length of cables within 100 km from each seamount. About 50% (n= 232) of the seamounts have at least 50 km of submarine cables within their radii, and approximately 17% of seamounts (n= 78) expose more than 1000 km of cables each. The seamounts with higher exposure are within the EEZs of Taiwan, Philippines and Vietnam, with Taiwanese volcanoes exposing more than 2500 km of cables each (Fig. 4, Fig. S2).

Ship traffic density also shows the highest values around Taiwanese seamounts (Fig. 4, Fig. S2), with the busiest areas including the Taiwanese strait, western and eastern portions of the northern South China Sea (east of Vietnam and west of Philippines), Singapore and Malacca Straits, and Gulf of Thailand, with the last three having zero exposure due to lack of known seamounts nearby. Krakatau also ranks high for ship traffic exposure (11^{th}).

In Figure 5, we aggregated exposure to the country level for individual seamount growth stages, and we found that 5 of the 11 EEZs in the region lie within 100 km of a volcanic seamount (India, Indonesia, Philippines, Taiwan and Vietnam), in addition to the central portion of the northern South China Sea, which is contended across different nations (i.e. here referred to as *overlapping claim waters*) and not discussed here. For population, Taiwan is the country with the highest exposure values (up to nearly 10M people), followed by Indonesia (up to 8M) and the Philippines (< 1M). For exposure of submarine cables, Taiwan and the Philippines rank the highest (up to >2,000 km of cables nearby seamounts), followed by Vietnam, and the other EEZs having similar values, with overall less than ~1,500 km of cables within their maritime boarders. For ship traffic density, again, Taiwan reports the highest exposure, followed by the Philippines, Indonesia, Vietnam and India, with similar values respectively. When considering the growth stage, besides being the country with the highest exposure values, Taiwan is also the country with exposure to the seamounts with higher rank (stage 3 and stage 4), and this is shown for all the assets considered.

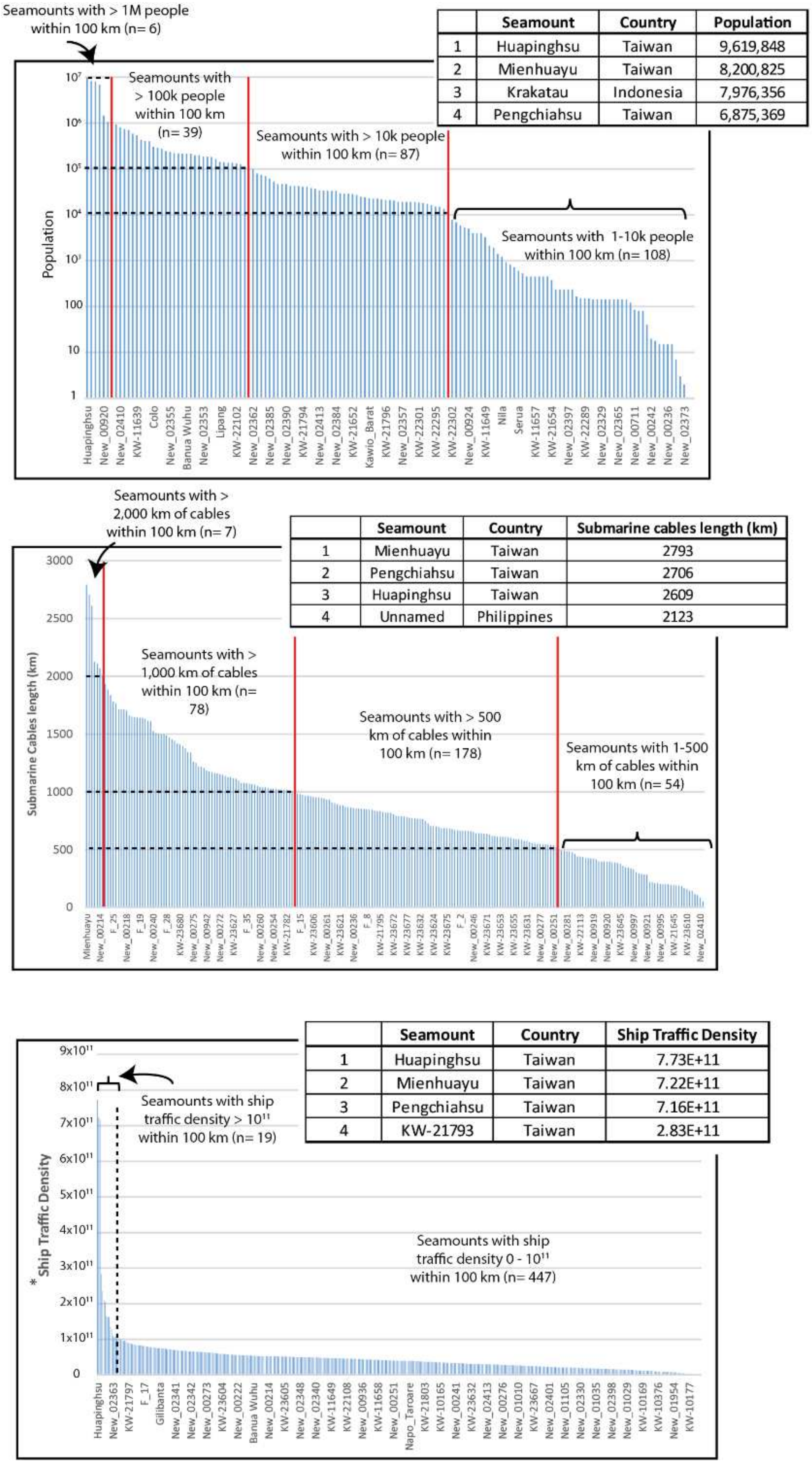

Figure 4. Exposure potential for population (top panel), submarine communication cables (middle panel) and ship traffic density (bottom panel) within 100 km from seamounts in and around SEA. Tables with the top 4 seamounts for exposure are also reported (full seamounts exposure lists are available as additional material; Table S1).

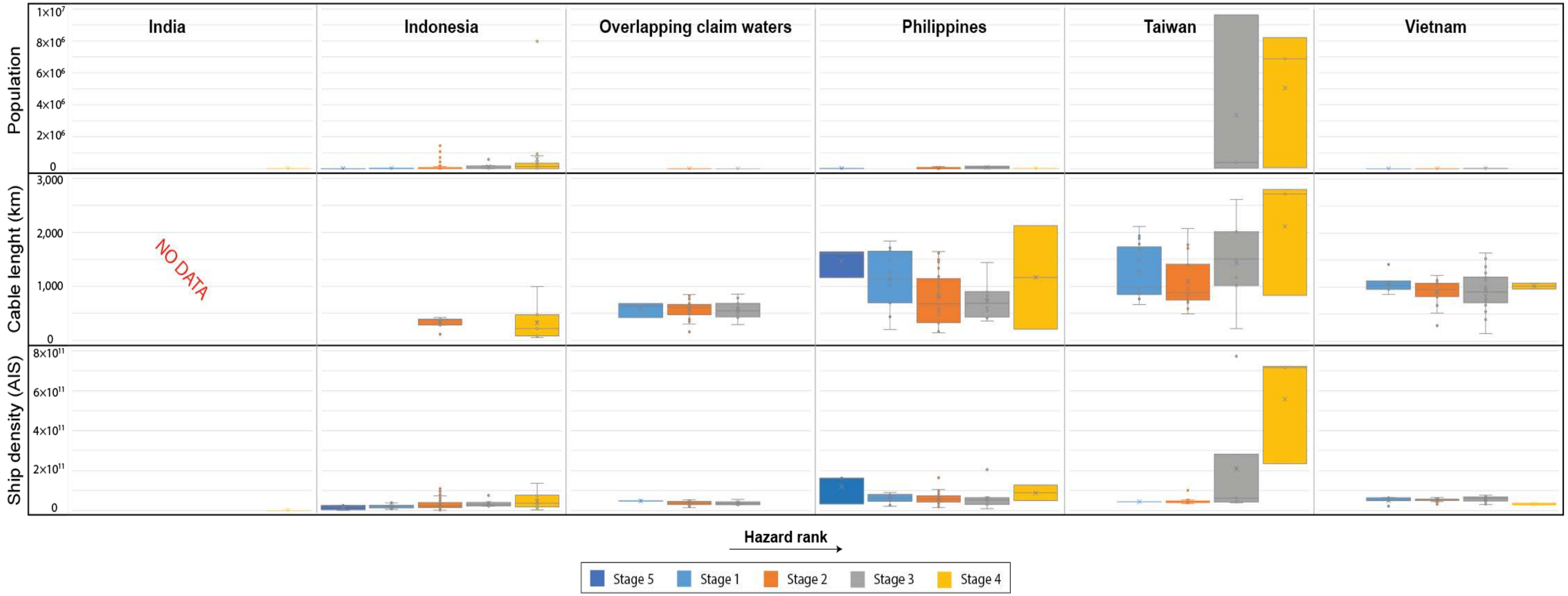

Figure 5. Exposure potential by country across all stages (ordered from left to right with increasing hazard rank), for population, submarine cables, and ship traffic density. Note that there is no cable data for India's seamounts

4.2.2. Hazard weighted seamount density (semi-quantitative)

Here we conducted a weighted Kernel Density Estimation (KDE) to understand which regions have higher potential to produce hazards from a seamount. This estimation is purposely weighted towards the more hazardous seamounts (Stage 3 and 4) (more details about the weighting process are reported in the methods section). A sensitivity analysis was run with only stage 3 and 4 seamounts to test the effect of the lower-weighted stage 1, 2 and 5 seamounts, which represent the majority of the seamounts in our study, on the final weighted density map. Their effect was found to be negligible (Fig. S2, Supplementary material), therefore we proceeded with this approach by including all seamount stages with a given hazard weight (Table 1). The results (Fig. 6) show that there are two large regions of interest, the largest is located in the South China Sea, followed by the Banda Sea. Other areas of interest, but with lower density, include the Celebes Sea, the Halmahera Sea, and the portion of Pacific Ocean just east of Taiwan and northern Philippines. Countries surrounding the areas with higher weighted density include southern Vietnam, southern and northern Philippines, and eastern Indonesia (Sulawesi, Maluku, and Lesser Sunda Islands).

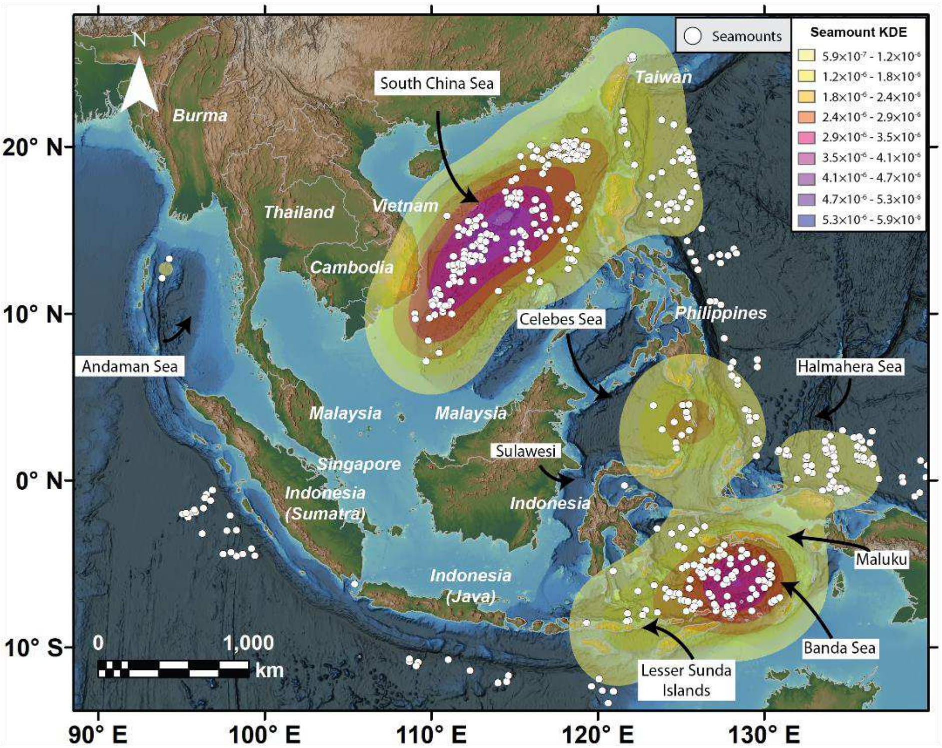

Figure 6. Hazard-weighted seamount density map in the region of interest. In dark purple the area with higher density of seamounts of higher hazard (see Table 1 for hazard weight).

5 Discussion

5.1 Potential sources of volcanic and related hazards in Southeast Asia and its surroundings

Our morphological assessment, although we did not consider geological, absolute age, and frequency/magnitude information in our seamount assessment (see discussion in later sections), can still provide insights about past and potentially future seamount behaviour. This can be used to narrow down the search of possible hazardous seamounts to investigate further in future studies as discussed below.

Mienhuayu and Pengchiahsu (offshore north of Taiwan), are two stage 4 simple cones, which lie in waters shallower than 200 m, with their summits just above sea level (16 and 49 m a.s.l. respectively). We can hypothesise that simple cones found in shallow waters in our region of interest are likely relatively young, because the sea level rose about 120 m over the last ~20k years (Diekmann et al., 2008; Hanebuth et al., 2011). If volcanoes that are now in shallow water environments were already existing 20k ago, we could assume that they were at least partially above water, and this would be reflected in their shape (e.g. presence of prominent terraces on the flanks). Mienhuayu and Pengchiahsu, which have their base at ~200 m b.s.l., and are considered Pleistocene in Age (100 ka or younger: Global Volcanism Program 2013), would be good case studies to test this hypothesis, however, the current available resolution prevents us from providing reliable inferences at this stage. Focused bathymetric and/or seismic surveys around these volcanoes would provide key clues about their relative age (older or younger than the last glacial maximum, 25 ka). This is important for hazard assessment, because Mienhuayu and Pengchiahsu are 50-60 km of the Taiwanese mainland and are among the volcanoes that rank the highest in the quantitative exposure potential analysis for all the assets considered (Fig. 4) (more discussion in the following sections).

The Kawio Barat seamount (~100 km south of the Philippines; Lat: 4.68°, Long: 125.09°) is a large simple cone rising from about 5,500 m b.s.l. up to ~2000 m b.s.l. (stage 2); it is unlikely that such a high seamount was formed in a single or short-lived eruptive event. Its regular conical shape, its height and the relatively steep slope angles (up to >30°) suggest a past explosive or mixed explosive/effusive history, as observed at similar cones on land; therefore, it represents another candidate to attention for future studies.

In this study Krakatau has been classified as a composite and stage 4 seamount, even though it is the newest cone formed as part of a caldera complex. It is well known for the 2018 eruption collapse-tsunami event (Self, 1992), and for the catastrophic eruption of its predecessor in 1883, which produced PDCs and tsunamis, killing over 30,000 people (Self, 1992). An example of a less known but still potentially hazardous composite and stage 4 seamount in the region is North Kawio, Indonesia (northern portion of the Sangihe volcanic arc; Lat: 4.68°, Long: 125.47°). This seamount is reported as Pleistocene in the GVP, but no other information about age is provided. It is a mostly submerged edifice, with multiple peaks above sea level (e.g. Marore, Kawio, and Kamboreng islands) and several submarine vents, covering a total area of about 1,500 km^2. These characteristics (distributed volcanism), besides the unknown and possibly relatively young age, and the relatively close proximity to mainland southern Philippines (~100 km south), make North Kawio a potential seamount to attention for tephra and tsunami hazards.

In terms of potentially more explosive submarine eruptions, calderas are key morphotypes to consider for the region. In our classification we identified 4 calderas, 3 of which have their summit at a water depth larger than ~1,300 m, with 2 of them being deeper than 2,000 m (all stage 2). Some calderas may form due to gradual subsidence over a longer period of time, hence not associated with any catastrophic explosive event. One key morphological indicator of either sudden or gradual collapse may be hidden in the intra-caldera slope angles; steep inner flanks may indicate a sudden sub-vertical movement downward resulting from the magma withdrawal from a shallow magma chamber. Despite the long-believed concept that explosive volcanic activity is hindered at large water depths (Cas, 1992), we show in our study that deep calderas with explosive features do exist. Seamount KW-23612, in the northern South China Sea (Fig. 2c), for example, despite having its rims reaching about 230 m b.s.l. (stage 3), has the caldera floor at over 2,000 m b.s.l., with inner slope angles up to ~50°. It is unlikely that such a depression (nearly 2,000 m deep), with such steep caldera walls was formed by gradual subsidence. Similarly, the recent eruption at the Hunga volcano, was responsible for deepening its caldera floor from an initial depth of about 200 m to about 850 m (Ribo et al., 2023). The eruption, although initiated at shallow water depth, was responsible for the withdrawal of intra-caldera material up to >800 m through explosive mechanisms, and this has important implications, once again, about the water depth limit of volcanic explosive eruptions. It is clear that explosive activity associated with caldera formation can be of rather large magnitude, resulting in high hazardous scenarios, particularly if this occurs in highly populated areas such as the South China Sea (e.g. seamounts KW-23612, New-00258) or off the coasts of Indonesia (seamount KW-10401).

5.2 Potential of multibeam high-resolution image analysis

As part of the seamount characterisation, and where multibeam high-resolution (90-m/pixel) bathymetry data were available, we searched for morphological features on and around seamounts that may give us clues about past hazards (examples reported in Figure 7). Note that this information is reported here for discussion purposes only, rather than for quantitative assessment of frequency and type of these past events because multibeam data only covers < 10% of the region of interest, which may bias the results.

From our investigation, we identified several debris avalanche deposits, landslide scars and slumps, explosive craters at depth, new potential seamounts, and deposits associated with submarine explosive volcanic activity. In order to understand the potential of such past hazards, and the impact they would have if they occurred nowadays, we highlight an example of a large landslide scar and associated deposit near Kawio Barat seamount, in the Celebes Sea, ~100 km south of Mindanao and 90 km north of Sangihe Island, Indonesia (Fig. 7b). We roughly estimated the debris avalanche volume from the topographic contours (through Esri®ArcMap™ 10.7.1), which resulted in a volume of ~14 km^3 of material; the deposit includes visible blocks (i.e. hummocks) up to ~500 m in diameter, which are typical of massive sector collapses (Violante et al., 2003; Idárraga-García and León, 2019; Carter et al., 2020). For comparison, the sector collapse of Mt Krakatau, Indonesia, in 2018, was about 0.15 km^3, which produced a local tsunami with maximum run-up of up to 14 m, and caused over 430 fatalities and millions of USD damage (Paris et al., 2020 and references therein). The event considered here is likely two orders of magnitude larger than the Krakatau event, and although the associated potential tsunami hazard cannot be compared directly because of bathymetric differences at both sites, the size of this event in the Sangihe arc gives us an idea of the relative scale.

Slumps are generally considered less likely to produce significant tsunamis, however, in some instances they have been inferred as the main cause of devastating tsunamis, such as the 1998 Papua New Guinea event (Okal and Synolakis, 2003; Brune et al., 2010). Subaqueous slumps appear as transverse ridges with steep toes and block of various sizes, as have been observed from bathymetric surveys around Hawaii (Moore et al., 1989), and differently from debris avalanche, they are not associated with any amphitheatre-like detachment area. An example is shown in Fig. 7a, where an area of over 100 km^2 of slumped material is highlighted, just north of seamount New-00919.

Explosive craters provide evidence of volcanic hazards; in Figure 7c we report an example from seamount KW-21797, ~300 km east-southeast of Taiwan and ~400 km northeast of Luzon, which is a composite and stage 2 seamount, and has a prominent topographic relief with a circular depression at the base of its NW side. This topographic feature is at a water depth of about 4,600 m, has a crater diameter of approximately 1.5 km and is around 150 m deep. We interpret this structure as a possible explosive crater because of its relatively large crater diameter and rather regular circular shape, which may have been formed by an individual explosive event. To the west of this structure, we identified an apron-like morphology extending westward for about 4 km, which is likely the volcanic deposit associated with this explosive structure mantling its flank. We cannot rule out the possibility that this structure and associated deposit may be related to effusive activity forming a westward lava flow. Evidence of explosive volcanism at water depths ≥ 1000 m is not new to geoscientists. Several examples are reported in literature, both along volcanic arcs (Murch et al., 2019b), mid-ocean ridges (Sohn et al., 2008), and hotspots (Schipper et al., 2010). Additionally, the potential occurrence of explosive deep-sea volcanic eruptions has been proved through analogue experiments (Dürig et al., 2020; Newland et al., 2022; Head and Wilson, 2003).

In the same area of seamount KW-21797, we identified other possible seamounts (Fig. 7d) that are not reported in any official dataset. They present themselves as individual composite edifices or chains of composite edifices (at least 3 chains can be recognised, all extending along W-E trends). These potential seamounts vary in height from < 500 m to ~1500 m, and their summit reaches water depths of ~5,500 to ~4,000 m b.s.l. Although all these seamounts have their summit in deep waters, some of them are higher than 1,000 m (stage 2). We do not include them in SEATANI as we cannot be sure that they are volcanic, but they may be worth further investigation.

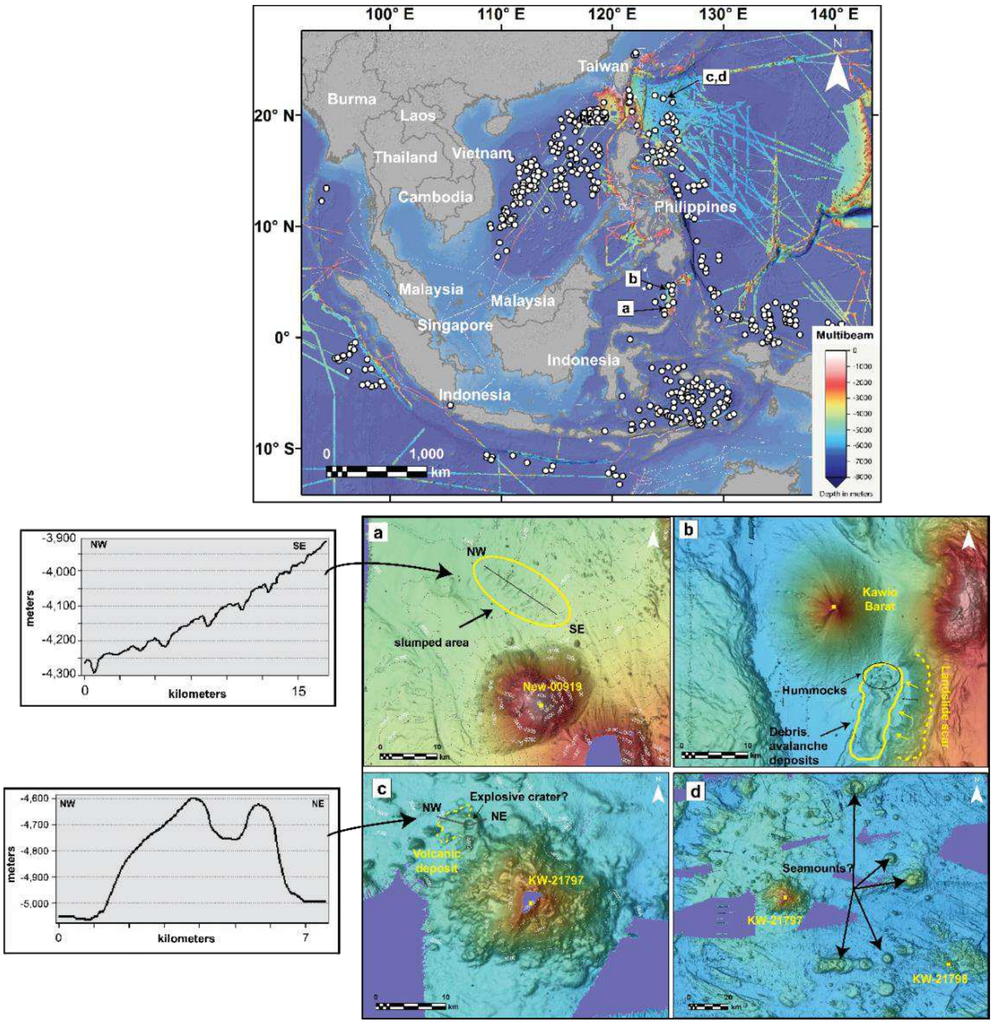

Figure 7. Map of the study region with multibeam data coverage (top panel), and relevant hazard features at some of the seamounts investigated, where multibeam data were available (bottom panels, a to d). Two bathymetric profiles for box a) and c) are also shown.

5.3 Potential areas of interest

Our seamount characterisation and exposure potential analyses highlights areas potentially more exposed to hazards in case of submarine eruption in and around SEA. Taiwan seems to be the candidate that requires more attention. It ranks high for both exposure analysis types conducted here. It has the highest number of people exposed, with two stage 4 and one stage 3 seamount (the most hazardous types) just 30-60 km northeast of the highly populated Taipei District (>9 M people). A submarine eruption at such distances may affect the nearby Taiwan through tephra falls and tsunamis. Subaqueous landslides, PDCs, or lava flows can damage the dense submarine cables array both north and south of Taiwan. Both volcanic and tsunami hazards can affect local ship traffic, which seems to be the densest in the whole region, with key connection between Taiwan and the rest of the region through eight major ports.

Besides Taiwan, if we consider the exposure by number and type of seamount by country (Fig. 5), Indonesia, Philippines and Vietnam are potentially threatened too. For Indonesia, the well-known Krakatau represents a hazard for population (~8 M people) and ship traffic, being a key passage to the South China Sea from the southern Indian Ocean. Eastern Indonesia (Sulawesi, Maluku and Lesser Sunda Island) is mostly exposed to stage 4, stage 3, and stage 2 seamounts. The Philippines is highly exposed as well, with the maximum exposures in the north (submarine cables, coasts), west (ship traffic) and south (coasts). Vietnam is characterised by high ship traffic density, with major commercial areas including the Mekong delta and Da Nang port. The Vietnam EEZ encloses a seamount that erupted in historical time, Ile des Cendres, 1923 (~115 km off the southeast coasts of Vietnam; Lat: 10.16°, Lon: 109.01). The eruption formed two islands (eroded soon after the eruption and now completely underwater) and at least another submarine cone (Global Volcanism Program, 2013). There is not much information about the eruption, but it was thought to be VEI= 2, and a local tsunami along the SE coasts of mainland Vietnam was also reported (Vu, 2008; Dai Dien, 2010). To our knowledge, there is no detailed study of the Ile Des Cendres complex, despite it representing the latest episode of submarine volcanism in the region and having a distributed nature (formation of several vents), which increases the area from which a potential eruption may occur, hence the hazard.

In areas of low seamount density and apparent lower hazard - for example the Indian EEZ (Andaman Sea, between Sumatra and Burma), which contains just two seamounts, both stage 4 - tsunami can potentially affect wider areas, such as the coasts of Thailand, Malaysia, Burma, Indonesia (Sumatra), India and, depending on the magnitude of the event, the coast of Singapore through the Malacca Strait. One of these seamounts is Barren Island, which shows past evidence of sector collapse (Chandrasekharam et al., 2009). Given the tectonic setting of these two volcanoes (submarine continuation of the Indonesian volcanic arc), we may expect the presence of other seamounts in this area not currently charted, hence potential increased hazard extent.

5.3.1 The geodynamic context for SEATANI seamounts

We noted that geology, absolute age, and eruption frequency/magnitude, were not taken into account for our hazard-exposure potential assessment, because of the lack of information for most of the seamounts in the region. Notwithstanding, in this section we discuss the geodynamic context of the SEATANI seamounts from a regional perspective, with a particular focus on the two regions that we found to host the highest number of stage 3 and 4, hence potentially more hazardous, seamounts: the South China Sea and the Banda Sea.

There are a number of seamounts (Fig. 6) in proximity to the Indonesian and Philippines trenches that show zero to very low weighted density, and this reflects their relatively low hazard potential. Seamounts in these particular tectonic settings are likely millions of years old and no longer active, being at the end of their cycle and approaching a subduction zone (Staudigel and Clague, 2010). It is likely that also some seamounts in the high weighted density regions of the South China Sea and Banda Sea may have been extinct for millions of years, however, these areas represent different tectonic settings, and must be discussed separately.

The South China Sea is the result of a multiphase continental rifting and breakup from the Eocene to the Miocene (e.g. Franke, 2013). Many studies provide evidence for extensive intraplate volcanism in the South China Sea following the end of the continental rifting (e.g. Xia et al., 2018; Gao et al., 2019; Zhao et al., 2020), with abundance of Late Cenozoic OIB-type basalts, inferred to be linked to a mantle plume (Yang et al., 2019). A more recent study identified widespread and partially still ongoing hydrothermal activity in the northern South China Sea, thought to be associated with magma intrusion (Zhao et al., 2021). On the southwestern edge of the South China Sea, east of southern Vietnam, there is a submarine volcano that erupted in historical times, Ile des Cendres, 1923. The volcano is located in proximity to a major regional fault, the East Vietnam Fault (Hall and Morley, 2004; Li et al., 2013) (Fig. 1); other major faults exist in the region (Mae Ping Fault and Three Pagogas Fault (Hall and Morley, 2004; Li et al., 2013), Fig. 1), and others may not be mapped, together with volcanoes in their proximity. Therefore, despite the intraplate setting, volcanism in the South China Sea may still play a role for future hazardous scenarios for the region.

The Banda Sea, on the other hand, results from more complex dynamics. This area was formed by the initial collision between the Australian and the Banda arc (which was already active from ~12 Ma, (Yang et al., 2021), and subsequent slab rollback, which created the extensional Banda Sea backarc basin (Wei et al., 2023). Therefore, seamounts in this area belong to at least two different formation mechanisms, arc volcanism and backarc extensional volcanism. If we consider the seamount growth stage for this area (Fig. 3b), we notice that that majority of seamounts along the Banda arc are stage 3 and 4, while the seamounts in the central portion of the Banda Sea basin are stage 2. Most of these stage 2 seamounts are likely as old or older than 3 Ma, given the inference that volcanism in the Sunda backarc basin ceased about 3 Ma (Honthaas et al., 1998), however, some of the Sunda arc seamounts (i.e. Banda Api, Serua, Nila, and Teon) are reported in the GVP, and erupted in recent times (within the last ~120 years). Other seamounts are found along this arc and include a stage 3 (New-02400) and a stage 4 (New-02393) seamount. Although we lack geological information from these two volcanoes, their tectonic setting and proximity to other active seamounts may suggest that they were active in relatively recent times and may still present a potential threat for the region in case of eruption.

5.4 Limitations and future goals

A major limitation of this study is the fact that we characterise the hazard potential from seamounts solely based on morphological (morphotype) and structural information (i.e. water depths, heights), with the high likelihood of including volcanoes that might have been inactive for millions of years, in turn resulting in an overestimation of the hazard potential. Despite this, the present study is relevant because it provides the elements to narrow down the research for future hazard studies from submarine volcanic activity in and around SEA.

When it comes to explosive versus effusive behaviour of a given volcano, hence the type of hazards it can produce, magma composition is a key aspect to consider. In subaerial environments, more silicic magmas are generally more explosive than basaltic magmas. However, in subaqueous environments the interaction between external water and magma is often consider the leading trigger of the explosivity of that particular volcano (e.g. Verolino et al., 2018, 2019). Many pioneer studies on the topic proved that this explosive interaction is more likely to occur with basaltic magmas (e.g. Wohletz, 1983, 1986; Büttner and Zimanowski, 1998), nevertheless, it also occurs with more silicic compositions (e.g. Austin-Erickson et al., 2008; Dürig et al., 2020). Magma composition was not accounted for in our assessment of hazard-exposure potential for two main reasons: 1) Only GVP seamounts have known composition (despite it could be assumed for some of the seamounts based on their tectonic setting); And 2) explosivity in subaqueous settings have been observed/inferred across all compositional domains, hence producing similar hazards regardless of composition. However, one difference is the production of pumice rafts in silicic eruptions (e.g. Havre, 2012; Fukutoku-Oka-no-Ba, 2021; Carey et al., 2014; Maeno et al., 2022), which is not expected for basaltic eruptions. Magma composition, eruption dynamics, and environmental factors that affect hazard extent, distribution and intensity, such as wind conditions or bathymetry, should be accounted for in future quantitative hazard studies for the region, once more information is made available.

Two main issues about the study of seamounts globally and regionally are that 1) the detection from space is limited within continental margins, and 2) the currently available bathymetry resolution is not enough to allow a comprehensive morphological characterisation of seamounts. As a result, we end up with large areas without seamounts (e.g. Sunda shelf), and many unclassified seamounts (n= 171). The general lack of seamounts on the Sunda shelf is questionable. Ile des Cendres and Veteran, besides other volcanoes not reported in this study because not in line with the definition of seamount used here (e.g. Ly Son group, Table S2), are in close proximity with a major regional fault, the East Vietnam Fault. Since this fault extends across the central-eastern portion of the Sunda shelf (all the way south to Borneo inland) (Li et al., 2013), it would not be surprising to have other volcanoes along or near to this fault zone. Other major faults mapped on the Sunda shelf include the Wang Chao (Hall and Morley, 2004) and Three Pagogas faults (Li et al., 2013), but no seamount is known to exist around these areas. The number and type of seamounts potentially not mapped and not considered for this study, may bias our results, particularly with regards to the KDE assessment. Potentially, the threat to countries not currently considered exposed, e.g. Singapore, is much greater than currently appreciated, because of the lack of continental shelf mapped seamounts. However, once again, we emphasize that here we did not produce any volcanic hazard maps for the region, but rather conducted a simple but necessary assessment of hazard and exposure potential, highlighting seamounts and areas of interest that can be the focus for more-in-depth studies.

For the quantitative exposure analysis, we used a 100 km radius around each seamount to indicate areas that may be impacted by volcanic activity. However, concentric radii, despite used in previous hazard studies, are not a strong approximation of how volcanic hazards behave (Jenkins et al., 2022): some hazards may affect areas smaller (e.g. lava flows, PDCs) or larger than the 100 km radius (e.g. tephra fall, pumice rafts).

Another limitation regards the exact location of submarine communication cables and how many people rely on this technology. The communication companies provide station to station information, which means that the exact path of each cable may not be as reported, and this probably partially affects our exposure results. Additionally, all countries in our study region depend on submarine cables for internet use, which translates into over 600 million of people in the region, however, the cable length analysed here does not give a direct information on the potential impact from a submarine volcanic eruption, which would be provided, for example, by the exact number of people that rely on specific cables per country. Despite this limitation, the direct relationship of seamount and cable density in some areas (northern South China Sea, Luzon Strait, East China Sea) is rather obvious (Fig. S2), and should be accounted for with regards to future cable installations in the region.

The above limitations can be overcome in different ways. First of all, we would need to improve our collaborative effort with private and government agencies, which may have seismic and bathymetry data that may improve our understanding of volcanic hazards from submarine volcanoes in the region. Second, we can partially improve the existing bathymetry datasets, by combining direct bathymetric information from Gebco and from local nautical charts (Felix et al., 2022), this will help with a better regional seamount characterisation, hazard assessment, and eventually hazard modelling and impact analysis at key locations. Third, we will use new satellite altimetry data of the sea surface, which will be made available from NASA in 2023 through the SWOT (Surface Water and Ocean Topography) mission, which was launched in December 2022. These new data will provide unprecedented resolutions of the sea surface, which in turn will be used to estimate location of smaller seamount than those currently detectable from satellite-derived methods, at a global scale. These data will be combined with the bathymetry data for more comprehensive analyses of hazard. Lastly, the results reported in this work, in addition to new data, will provide an evidence base for more focused investigations to be conducted at potentially high threatening seamounts (including sampling through Remotely Operated Vehicles, and later laboratory analysis for a complete characterisation). This will serve countries across the region to become more prepared and resilient against submarine volcanic hazards.

6 Conclusions

Seamounts are an understudied and potentially silent threat for human populations and infrastructure. Despite the global identification of about 35,000 seamounts (Gevorgian et al., 2023), only a few of them are thoroughly studied and monitored (e.g. Deardorff et al., 2011; Caress et al., 2012; Carey et al., 2014; Berthod et al., 2021). We conducted a seamount characterisation and associated hazard-exposure potential assessment on a regional scale for SEA and surrounding areas, through the SEATANI dataset, which provides the basis for more focused investigations of hazards for the region in the near future at key locations. Our results show that composite and stage 2 seamounts are the most abundant in the region, however, stage 3 and stage 4 seamounts (simple, composite and calderas) are the most important for hazard potential and numbers of people, lengths of cable and density of shipping exposed. Taiwan is the country with the highest total exposure potential (across all exposure types) within 100 km of volcanic seamounts, followed by Indonesia, Philippines and Vietnam. The hazard-weighted seamount density assessment highlights two main areas of interest: the northern South China Sea and the Banda Sea. Any volcanic and related hazards (e.g. tsunamis), if generated in these areas, will potentially affect the coasts of Southern Taiwan, northern and southern Philippines, Vietnam and eastern Indonesia.

This work represents the first step towards understanding the threat that submarine volcanoes pose to populations and infrastructure in and around SEA. The integration of new bathymetry, seismic and satellite-derived altimetry data (i.e. SWOT mission) will shed more light on the potential of these volcanoes and enhance awareness, preparedness and resilience for the countries surrounding these waters.

Data availability

Data are available in the supplementary material files and in the public data repository of NTU (https://researchdata.ntu.edu.sg/privateurl.xhtml?token=820ea7c9-4ff4-48f8-8e8b-98cd4ffe01f8)

References

Austin-Erickson, A., Büttner, R., Dellino, P., Ort, M. H., and Zimanowski, B.: Phreatomagmatic explosions of rhyolitic magma: Experimental and field evidence, J. Geophys. Res., 113, B11201, https://doi.org/10.1029/2008JB005731, 2008.

Berthod, C., Médard, E., Bachèlery, P., Gurioli, L., Di Muro, A., Peltier, A., Komorowski, J.-C., Benbakkar, M., Devidal, J.-L., Langlade, J., Besson, P., Boudon, G., Rose-Koga, E., Deplus, C., Le Friant, A., Bickert, M., Nowak, S., Thinon, I., Burckel, P., Hidalgo, S., Kaliwoda, M., Jorry, S. J., Fouquet, Y., and Feuillet, N.: The 2018-ongoing Mayotte submarine eruption: Magma migration imaged by petrological monitoring, Earth and Planetary Science Letters, 571, 117085, https://doi.org/10.1016/j.epsl.2021.117085, 2021.

Brown, S. K., Sparks, R. S. J., and Jenkins, S. F.: Global distribution of volcanic threat, in: Global Volcanic Hazards and Risk, edited by: Loughlin, S. C., Sparks, S., Brown, S. K., Jenkins, S. F., and Vye-Brown, C., Cambridge University Press, 359–370, https://doi.org/10.1017/CBO9781316276273.025, 2015.

Brune, S., Babeyko, A. Y., Gaedicke, C., and Ladage, S.: Hazard assessment of underwater landslide-generated tsunamis: a case study in the Padang region, Indonesia, Nat Hazards, 53, 205–218, https://doi.org/10.1007/s11069-009-9424-x, 2010.

Büttner, R. and Zimanowski, B.: Physics of thermohydraulic explosions, Phys. Rev. E, 57, 5726–5729, https://doi.org/10.1103/PhysRevE.57.5726, 1998.

Caress, D. W., Clague, D. A., Paduan, J. B., Martin, J. F., Dreyer, B. M., Chadwick, W. W., Denny, A., and Kelley, D. S.: Repeat bathymetric surveys at 1-metre resolution of lava flows erupted at Axial Seamount in April 2011, Nature Geosci, 5, 483–488, https://doi.org/10.1038/ngeo1496, 2012.

Carey, R. J., Wysoczanski, R., Wunderman, R., and Jutzeler, M.: Discovery of the Largest Historic Silicic Submarine Eruption, Eos, Transactions American Geophysical Union, 95, 157–159, https://doi.org/10.1002/2014EO190001, 2014.

Carter, G. D. O., Cooper, R., Gafeira, J., Howe, J. A., and Long, D.: Morphology of small-scale submarine mass movement events across the northwest United Kingdom, Geomorphology, 365, 107282, https://doi.org/10.1016/j.geomorph.2020.107282, 2020.

Cas, R. A. F.: Submarine volcanism; eruption styles, products, and relevance to understanding the host-rock successions to volcanic-hosted massive sulfide deposits, Economic Geology, 87, 511–541, https://doi.org/10.2113/gsecongeo.87.3.511, 1992.

Chadwick, W. W., Cashman, K. V., Embley, R. W., Matsumoto, H., Dziak, R. P., de Ronde, C. E. J., Lau, T. K., Deardorff, N. D., and Merle, S. G.: Direct video and hydrophone observations of submarine explosive eruptions at NW Rota-1 volcano, Mariana arc: SUBMARINE EXPLOSIVE ERUPTIONS AT NW ROTA-1, J. Geophys. Res., 113, https://doi.org/10.1029/2007JB005215, 2008.

Chandrasekharam, D., Santo, A. P., Capaccioni, B., Vaselli, O., Alam, M. A., Manetti, P., and Tassi, F.: Volcanological and petrological evolution of Barren Island (Andaman Sea, Indian Ocean), Journal of Asian Earth Sciences, 35, 469–487, https://doi.org/10.1016/j.jseaes.2009.02.010, 2009.

Clague, D. A., Holcomb, R. T., Sinton, J. M., Detrick, R. S., and Torresan, M. E.: Pliocene and Pleistocene alkalic flood basalts on the seafloor north of the Hawaiian islands, Earth and Planetary Science Letters, 98, 175–191, https://doi.org/10.1016/0012-821X(90)90058-6, 1990.

Clague, D. A., Paduan, J. B., Caress, D. W., Thomas, H., Chadwick Jr., W. W., and Merle, S. G.: Volcanic morphology of West Mata Volcano, NE Lau Basin, based on high-resolution bathymetry and depth changes, Geochemistry, Geophysics, Geosystems, 12, https://doi.org/10.1029/2011GC003791, 2011.

Clague, D. A., Dreyer, B. M., Paduan, J. B., Martin, J. F., Chadwick, W. W., Caress, D. W., Portner, R. A., Guilderson, T. P., McGann, M. L., Thomas, H., Butterfield, D. A., and Embley, R. W.: Geologic history of the summit of Axial Seamount, Juan de Fuca Ridge, Geochemistry, Geophysics, Geosystems, 14, 4403–4443, https://doi.org/10.1002/ggge.20240, 2013.

Dai Dien, L.: Overview on tsunami risk evaluation and NPP project in Vietnam. 1st Kawashiwazaki International Symposium on Seismic Safety of Nuclear Installations, 24–26 November 2010, NIIT, Niigata, Japan (http://www.nsr.go.jp/archive/jnes/ seismic-symposium10/presentationdata/3_sessionB/B-09.pdf)., 2010.

Deardorff, N. D., Cashman, K. V., and Chadwick, W. W.: Observations of eruptive plume dynamics and pyroclastic deposits from submarine explosive eruptions at NW Rota-1, Mariana arc, Journal of Volcanology and Geothermal Research, 202, 47–59, https://doi.org/10.1016/j.jvolgeores.2011.01.003, 2011.

Diekmann, B., Hofmann, J., Henrich, R., Fütterer, D. K., Röhl, U., and Wei, K.-Y.: Detrital sediment supply in the southern Okinawa Trough and its relation to sea-level and Kuroshio dynamics during the late Quaternary, Marine Geology, 255, 83–95, https://doi.org/10.1016/j.margeo.2008.08.001, 2008.

Dürig, T., White, J. D. L., Murch, A. P., Zimanowski, B., Büttner, R., Mele, D., Dellino, P., Carey, R. J., Schmidt, L. S., and Spitznagel, N.: Deep-sea eruptions boosted by induced fuel–coolant explosions, Nat. Geosci., 13, 498–503, https://doi.org/10.1038/s41561-020-0603-4, 2020.

Dziak, R. P., Bohnenstiehl, D. R., Baker, E. T., Matsumoto, H., Caplan-Auerbach, J., Embley, R. W., Merle, S. G., Walker, S. L., Lau, T.-K., and Chadwick Jr., W. W.: Long-term explosive degassing and debris flow activity at West Mata submarine volcano, Geophysical Research Letters, 42, 1480–1487, https://doi.org/10.1002/2014GL062603, 2015.

Embley, R. W., Chadwick, W. W., Baker, E. T., Butterfield, D. A., Resing, J. A., de Ronde, C. E. J., Tunnicliffe, V., Lupton, J. E., Juniper, S. K., Rubin, K. H., Stern, R. J., Lebon, G. T., Nakamura, K., Merle, S. G., Hein, J. R., Wiens, D. A., and Tamura, Y.: Long-term eruptive activity at a submarine arc volcano, Nature, 441, 494–497, https://doi.org/10.1038/nature04762, 2006.

Fan, C., Xia, S., Zhao, F., Sun, J., Cao, J., Xu, H., and Wan, K.: New insights into the magmatism in the northern margin of the South China Sea: Spatial features and volume of intraplate seamounts: INTRAPLATE SEAMOUNTS IN THE SCS, Geochem. Geophys. Geosyst., 18, 2216–2239, https://doi.org/10.1002/2016GC006792, 2017.

Felix, R. P., Hubbard, J. A., Bradley, K. E., Lythgoe, K. H., Li, L., and Switzer, A. D.: Tsunami hazard in Lombok and Bali, Indonesia, due to the Flores back-arc thrust, Nat. Hazards Earth Syst. Sci., 22, 1665–1682, https://doi.org/10.5194/nhess-22-1665-2022, 2022.

Feuillet, N., Jorry, S., Crawford, W. C., Deplus, C., Thinon, I., Jacques, E., Saurel, J. M., Lemoine, A., Paquet, F., Satriano, C., Aiken, C., Foix, O., Kowalski, P., Laurent, A., Rinnert, E., Cathalot, C., Donval, J.-P., Guyader, V., Gaillot, A., Scalabrin, C., Moreira, M., Peltier, A., Beauducel, F., Grandin, R., Ballu, V., Daniel, R., Pelleau, P., Gomez, J., Besançon, S., Geli, L., Bernard, P., Bachelery, P., Fouquet, Y., Bertil, D., Lemarchand, A., and Van der Woerd, J.: Birth of a large volcanic edifice offshore Mayotte via lithosphere-scale dyke intrusion, Nat. Geosci., 14, 787–795, https://doi.org/10.1038/s41561-021-00809-x, 2021.

Franke, D.: Rifting, lithosphere breakup and volcanism: Comparison of magma-poor and volcanic rifted margins, Marine and Petroleum Geology, 43, 63–87, https://doi.org/10.1016/j.marpetgeo.2012.11.003, 2013.

Gao, J., Bangs, N., Wu, S., Cai, G., Han, S., Ma, B., Wang, J., Xie, Y., Huang, W., Dong, D., and Wang, D.: Post-seafloor spreading magmatism and associated magmatic hydrothermal systems in the Xisha uplift region, northwestern South China Sea, Basin Res, 31, 688–708, https://doi.org/10.1111/bre.12338, 2019.

Gevorgian, J., Sandwell, D. T., Yu, Y., Kim, S., and Wessel, P.: Global Distribution and Morphology of Small Seamounts, Earth and Space Science, 10, e2022EA002331, https://doi.org/10.1029/2022EA002331, 2023.

Global Volcanism Program: Global Volcanism Program, 2013 (19 June 2021). Venzke, E (ed.). Smithsonian Institution. Downloaded 19 Jun 2021. https://volcano.si.edu/volcano.cfm?vn=275813, 2013.

Gusman, A. R., Roger, J., Noble, C., Wang, X., Power, W., and Burbidge, D.: The 2022 Hunga Tonga-Hunga Ha'apai Volcano Air-Wave Generated Tsunami, Pure Appl. Geophys., 179, 3511–3525, https://doi.org/10.1007/s00024-022-03154-1, 2022.

Hall, R. and Morley, C. K.: Sundaland basins, in: Geophysical Monograph Series, vol. 149, edited by: Clift, P., Kuhnt, W., Wang, P., and Hayes, D., American Geophysical Union, Washington, D. C., 55–85, https://doi.org/10.1029/149GM04, 2004.

Hammond, S. R.: Relationships between lava types, seafloor morphology, and the occurrence of hydrothermal venting in the ASHES Vent Field of Axial Volcano, Journal of Geophysical Research: Solid Earth, 95, 12875–12893, https://doi.org/10.1029/JB095iB08p12875, 1990.

Hamzah, L., Puspito, N. T., and Imamura, F.: Tsunami Catalog and Zones in Indonesia., Journal of Natural Disaster Science, 22, 25–43, https://doi.org/10.2328/jnds.22.25, 2000.

Hanebuth, T. J. J., Voris, H. K., Yokoyama, Y., Saito, Y., and Okuno, J.: Formation and fate of sedimentary depocentres on Southeast Asia's Sunda Shelf over the past sea-level cycle and biogeographic implications, Earth-Science Reviews, 104, 92–110, https://doi.org/10.1016/j.earscirev.2010.09.006, 2011.

Harders, R., Ranero, C. R., and Weinrebe, W.: Characterization of Submarine Landslide Complexes Offshore Costa Rica: An Evolutionary Model Related to Seamount Subduction. In S. Krastel et al. (eds.), Submarine Mass Movements and Their Consequences, Advances in Natural and Technological Hazards Research 37, DOI 10.1007/978-3-319-00972-8 34, © Springer International Publishing Switzerland 2014, 2014.

Head, J. W. and Wilson, L.: Deep submarine pyroclastic eruptions: theory and predicted landforms and deposits, Journal of Volcanology and Geothermal Research, 121, 155–193, https://doi.org/10.1016/S0377-0273(02)00425-0, 2003.

Hidayat, A., Marfai, M. A., and Hadmoko, D. S.: Eruption on Indonesia's volcanic islands: a review of potential hazards, fatalities, and management, IOP Conf. Ser.: Earth Environ. Sci., 485, 012061, https://doi.org/10.1088/1755-1315/485/1/012061, 2020.

Honthaas, C., Réhault, J.-P., Maury, R. C., Bellon, H., Hémond, C., Malod, J.-A., Cornée, J.-J., Villeneuve, M., Cotten, J., Burhanuddin, S., Guillou, H., and Arnaud, N.: A Neogene back-arc origin for the Banda Sea basins: geochemical and geochronological constraints from the Banda ridges (East Indonesia), Tectonophysics, 298, 297–317, https://doi.org/10.1016/S0040-1951(98)00190-5, 1998.

Idárraga-García, J. and León, H.: Unraveling the Underwater Morphological Features of Roncador Bank, Archipelago of San Andres, Providencia and Santa Catalina (Colombian Caribbean), Front. Mar. Sci., 6, 77, https://doi.org/10.3389/fmars.2019.00077, 2019.

Jenkins, S. F., Biass, S., Williams, G. T., Hayes, J. L., Tennant, E., Yang, Q., Burgos, V., Meredith, E. S., Lerner, G. A., Syarifuddin, M., and Verolino, A.: Evaluating and ranking Southeast Asia's exposure to explosive volcanic hazards, Nat. Hazards Earth Syst. Sci., 22, 1233–1265, https://doi.org/10.5194/nhess-22-1233-2022, 2022.

Jutzeler, M., Marsh, R., Carey, R. J., White, J. D. L., Talling, P. J., and Karlstrom, L.: On the fate of pumice rafts formed during the 2012 Havre submarine eruption, Nat Commun, 5, 3660, https://doi.org/10.1038/ncomms4660, 2014.

Kim, S.-S. and Wessel, P.: New global seamount census from altimetry-derived gravity data: New global seamount census, Geophysical Journal International, 186, 615–631, https://doi.org/10.1111/j.1365-246X.2011.05076.x, 2011.

Li, L., Clift, P. D., and Nguyen, H. T.: The sedimentary, magmatic and tectonic evolution of the southwestern South China Sea revealed by seismic stratigraphic analysis, Mar Geophys Res, 34, 341–365, https://doi.org/10.1007/s11001-013-9171-y, 2013.

Moore, J. G., Clague, D. A., Holcomb, R. T., Lipman, P. W., Normark, W. R., and Torresan, M. E.: Prodigious submarine landslides on the Hawaiian Ridge, Journal of Geophysical Research: Solid Earth, 94, 17465–17484, https://doi.org/10.1029/JB094iB12p17465, 1989.

Murch, A. P., White, J. D. L., and Carey, R. J.: Characteristics and Deposit Stratigraphy of Submarine-Erupted Silicic Ash, Havre Volcano, Kermadec Arc, New Zealand, Front. Earth Sci., 7, 1, https://doi.org/10.3389/feart.2019.00001, 2019a.

Murch, A. P., White, J. D. L., and Carey, R. J.: Unusual fluidal behavior of a silicic magma during fragmentation in a deep subaqueous eruption, Havre volcano, southwestern Pacific Ocean, Geology, 47, 487–490, https://doi.org/10.1130/G45657.1, 2019b.

Murch, A. P., Portner, R. A., Rubin, K. H., and Clague, D. A.: Deep-subaqueous implosive volcanism at West Mata seamount, Tonga, Earth and Planetary Science Letters, 578, 117328, https://doi.org/10.1016/j.epsl.2021.117328, 2022.

Mutaqin, B. W., Lavigne, F., Hadmoko, D. S., and Ngalawani, M. N.: Volcanic Eruption-Induced Tsunami in Indonesia: A Review, IOP Conf. Ser.: Earth Environ. Sci., 256, 012023, https://doi.org/10.1088/1755-1315/256/1/012023, 2019.

NCEI/WDS: National Geophysical Data Center / World Data Service: NCEI/WDS Global Historical Tsunami Database. NOAA National Centers for Environmental Information. doi:10.7289/V5PN93H7, n.d.

Newland, E. L., Mingotti, N., and Woods, A. W.: Dynamics of deep-submarine volcanic eruptions, Sci Rep, 12, 3276, https://doi.org/10.1038/s41598-022-07351-9, 2022.

Ohno, Y., Iguchi, A., Ijima, M., Yasumoto, K., and Suzuki, A.: Coastal ecological impacts from pumice rafts, Sci Rep, 12, 11187, https://doi.org/10.1038/s41598-022-14614-y, 2022.

Okal, E. A. and Synolakis, C. E.: Field survey and numerical simulations: a theoretical comparison of tsunamis from dislocations and landslides. Pure Appl Geophys 160:2177–2188, 2003.

Omira, R., Ramalho, I., Terrinha, P., Baptista, M. A., Batista, L., and Zitellini, N.: Deep-water seamounts, a potential source of tsunami generated by landslides? The Hirondelle Seamount, NE Atlantic, Marine Geology, 379, 267–280, https://doi.org/10.1016/j.margeo.2016.06.010, 2016.

Paris, A., Heinrich, P., Paris, R., and Abadie, S.: The December 22, 2018 Anak Krakatau, Indonesia, Landslide and Tsunami: Preliminary Modeling Results, Pure Appl. Geophys., 177, 571–590, https://doi.org/10.1007/s00024-019-02394-y, 2020.

Paris, R., Switzer, A. D., Belousova, M., Belousov, A., Ontowirjo, B., Whelley, P. L., and Ulvrova, M.: Volcanic tsunami: a review of source mechanisms, past events and hazards in Southeast Asia (Indonesia, Philippines, Papua New Guinea), Nat Hazards, 70, 447–470, https://doi.org/10.1007/s11069-013-0822-8, 2014.

Reyes-Hardy, M.-P., Aguilera Barraza, F., Sepúlveda Birke, J. P., Esquivel Cáceres, A., and Inostroza Pizarro, M.: GIS-based volcanic hazards, vulnerability and risks assessment of the Guallatiri Volcano, Arica y Parinacota Region, Chile, Journal of South American Earth Sciences, 109, 103262, https://doi.org/10.1016/j.jsames.2021.103262, 2021.

Ribo, M., Cronin, S., Stern, S., Park, S. H., Garvin, J., and Kula, T.: Morphological evolution of the Hunga Tonga–Hunga Ha‘apai submarine volcano after the explosive eruption (No. EGU23-17221). Copernicus Meetings., 2023.

Schipper, C. I., White, J. D. L., Houghton, B. F., Shimizu, N., and Stewart, R. B.: “Poseidic” explosive eruptions at Loihi Seamount, Hawaii, Geology, 38, 291–294, https://doi.org/10.1130/G30351.1, 2010.

Schmidt, R. A. L. F., Schmincke, H. U., and Sigurdsson, H.: Seamounts and island building. Encyclopedia of volcanoes, 383-402., 2000.

Schnur, S. R., Chadwick Jr., W. W., Embley, R. W., Ferrini, V. L., de Ronde, C. E. J., Cashman, K. V., Deardorff, N. D., Merle, S. G., Dziak, R. P., Haxel, J. H., and Matsumoto, H.: A decade of volcanic construction and destruction at the summit of NW Rota-1 seamount: 2004–2014, Journal of Geophysical Research: Solid Earth, 122, 1558–1584, https://doi.org/10.1002/2016JB013742, 2017.

Self, S.: Krakatau revisited: The course of events and interpretation of the 1883 eruption, GeoJournal, 28, https://doi.org/10.1007/BF00177223, 1992.

Sims, K., Reith, A., Bright, E., McKee, J., and Rose, A.: LandScan Global 2021 [Data set]. Oak Ridge National Laboratory. https://doi.org/10.48690/1527702, 2022.

Small, C. and Naumann, T.: The global distribution of human population and recent volcanism, Environmental Hazards, 3, 93–109, https://doi.org/10.3763/ehaz.2001.0309, 2001.

Sohn, R. A., Willis, C., Humphris, S., Shank, T. M., Singh, H., Edmonds, H. N., Kunz, C., Hedman, U., Helmke, E., Jakuba, M., Liljebladh, B., Linder, J., Murphy, C., Nakamura, K., Sato, T., Schlindwein, V., Stranne, C., Tausenfreund, M., Upchurch, L., Winsor, P., Jakobsson, M., and Soule, A.: Explosive volcanism on the ultraslow-spreading Gakkel ridge, Arctic Ocean, Nature, 453, 1236–1238, https://doi.org/10.1038/nature07075, 2008.

Speidel, U.: The Hunga Tonga Hunga Ha'apai Eruption – A Postmortem: What happened to Tonga's Internet in January 2022, and what lessons are there to be learned?, in: Proceedings of the 17th Asian Internet Engineering Conference, AINTEC'22: The 17th Asian Internet Engineering Conference, Hiroshima Japan, 70–78, https://doi.org/10.1145/3570748.3570759, 2022.

Staudigel, H. and Clague, D.: The Geological History of Deep-Sea Volcanoes: Biosphere, Hydrosphere, and Lithosphere Interactions, Oceanog., 23, 58–71, https://doi.org/10.5670/oceanog.2010.62, 2010.

Staudigel, H., Koppers, A. A. P., Lavelle, W., Pitcher, T. J., and Shank, T. M.: Defining the Word "Seamount," 2010.

Taha, G., Loughman, R., Colarco, P. R., Zhu, T., Thomason, L. W., and Jaross, G.: Tracking the 2022 Hunga Tonga-Hunga Ha'apai Aerosol Cloud in the Upper and Middle Stratosphere Using Space-Based Observations, Geophysical Research Letters, 49, https://doi.org/10.1029/2022GL100091, 2022.

TeleGeography: Worldwide submarine cables. https://services.arcgis.com/6DIQcwlPy8knb6sg/arcgis/rest/services/SubmarineCables/FeatureServer (Downloaded on 11 June 2021), n.d.

The World Bank: The January 15, 2022 Hunga Tonga-Hunga Ha'apai eruption and tsunami, Tonga Global Rapid Post Disaster Damage Estimation (Grade) Report. https://thedocs.worldbank.org/en/doc/b69af83e486aa652d4232276ad698c7b-0070062022/original/GRADE-Report-Tonga-Volcanic-Eruption.pdf, 2022.

The World Bank Group: Global Shipping Traffic Density. https://datacatalog.worldbank.org/search/dataset/0037580. Downloaded on 13 July 2021., n.d.

Verolino, A., White, J. D. L., and Brenna, M.: Eruption dynamics at Pahvant Butte volcano, Utah, western USA: insights from ash-sheet dispersal, grain size, and geochemical data, Bull Volcanol, 80, 1–18, https://doi.org/10.1007/s00445-018-1256-7, 2018.

Verolino, A., White, J. D. L., Dürig, T., and Cappuccio, F.: Black Point – Pyroclasts of a Surtseyan eruption show no change during edifice growth to the surface from 100 m water depth, Journal of Volcanology and Geothermal Research, 384, 85–102, https://doi.org/10.1016/j.jvolgeores.2019.07.013, 2019.

Verolino, A., Jenkins, S. F., Sieh, K., Herrin, J. S., Schonwalder-Angel, D., Sihavong, V., and Oh, J. H.: Assessing volcanic hazard and exposure to lava flows at remote volcanic fields: a case study from the Bolaven Volcanic Field, Laos, J Appl. Volcanol., 11, 6, https://doi.org/10.1186/s13617-022-00116-z, 2022a.

Verolino, A., White, J. D. L., Baxter, R. J. M., Schipper, C. I., and Thordarson, T.: Characteristics of Sub-Aerially Emplaced Pyroclasts in the Surtsey Eruption Deposits: Implications for Diverse Surtseyan Eruptive Styles, Geosciences, 12, 79, https://doi.org/10.3390/geosciences12020079, 2022b.

Violante, C., Budillon, F., Esposito, E., Porfido, S., and Vittori, E.: SUBMERGED HUMMOCKY TOPOGRAPHIES AND RELATIONS WITH LANDSLIDES. NORTHWESTERN FLANK OF ISCHIA IS-LAND, SOUTHERN ITALY, 2003.

Vu, T. C.: Earthquake and Tsunami Scenarios in the South China Sea (www.ims.nus.edu.sg/Programs/ocean07/files/vu1.ppt), 2008.

Wang, Q., Guo, J., Wang, Z., Tahchi, E., Wang, X., Moran, B., and Zukerman, M.: Cost-Effective Path Planning for Submarine Cable Network Extension, IEEE Access, 7, 61883–61895, https://doi.org/10.1109/ACCESS.2019.2915125, 2019.

Wei, X., Luan, X., Meng, F., Lu, Y., He, H., Qiao, J., Yin, J., Wang, Y., and Xue, Y.: Deformation feature and tectonic model of the Timor Trough: New interpretation of the evolution and mechanism of Banda arc-continent collision, Tectonophysics, 862, 229958, https://doi.org/10.1016/j.tecto.2023.229958, 2023.

Wessel, P.: Seamount Characteristics. In: Pitcher T, Morato T, et al., editors. Seamounts: Ecology, Fisheries, & Conservation. Fish and Aquatic Resources Series 12. Blackwell Publishing., p. 3-20., 2007.

Whelley, P. L., Newhall, C. G., and Bradley, K. E.: The frequency of explosive volcanic eruptions in Southeast Asia, Bull Volcanol, 77, 1, https://doi.org/10.1007/s00445-014-0893-8, 2015.

Wohletz, K. H.: Mechanisms of hydrovolcanic pyroclast formation: Grain-size, scanning electron microscopy, and experimental studies, 33, 1983.

Wohletz, K. H.: Explosive magma-water interactions: Thermodynamics, explosion mechanisms, and field studies, Bull Volcanol, 48, 245–264, https://doi.org/10.1007/BF01081754, 1986.

Xia, S., Zhao, F., Zhao, D., Fan, C., Wu, S., Mi, L., Sun, J., Cao, J., and Wan, K.: Crustal plumbing system of post-rift magmatism in the northern margin of South China Sea: New insights from integrated seismology, Tectonophysics, 744, 227–238, https://doi.org/10.1016/j.tecto.2018.07.002, 2018.

Yang, F., Huang, X.-L., Xu, Y.-G., and He, P.-L.: Plume-ridge interaction in the South China Sea: Thermometric evidence from Hole U1431E of IODP Expedition 349, Lithos, 324–325, 466–478, https://doi.org/10.1016/j.lithos.2018.11.031, 2019.

Yang, X., Singh, S. C., and Deighton, I.: The Margin-Oblique Kumawa Strike-Slip Fault in the Banda Forearc, East Indonesia: Structural Deformation, Tectonic Origin and Geohazard Implication, Tectonics, 40, https://doi.org/10.1029/2020TC006567, 2021.

Zhao, F., Alves, T. M., Xia, S., Li, W., Wang, L., Mi, L., Wu, S., Cao, J., and Fan, C.: Along-strike segmentation of the South China Sea margin imposed by inherited pre-rift basement structures, Earth and Planetary Science Letters, 530, 115862, https://doi.org/10.1016/j.epsl.2019.115862, 2020.

Zhao, F., Berndt, C., Alves, T. M., Xia, S., Li, L., Mi, L., and Fan, C.: Widespread hydrothermal vents and associated volcanism record prolonged Cenozoic magmatism in the South China Sea, GSA Bulletin, 133, 2645–2660, https://doi.org/10.1130/B35897.1, 2021.

Zorn, E. U., Orynbaikyzy, A., Plank, S., Babeyko, A., Darmawan, H., Robbany, I. F., and Walter, T. R.: Identification and ranking of subaerial volcanic tsunami hazard sources in Southeast Asia, Nat. Hazards Earth Syst. Sci., 22, 3083–3104, https://doi.org/10.5194/nhess-22-3083-2022, 2022.

Acknowledgements

We would like to thank the editor and reviewers for improving this manuscript. This research was supported by the Earth Observatory of Singapore via its funding from the National Research Foundation Singapore and the Singapore Ministry of Education under the Research Centers of Excellence initiative. This work comprises EOS contribution number 531.

Author contribution

AV: Paper conceptualisation and preparation, figures production, data elaboration, analysis and interpretation, editing; SFW: data elaboration, analysis and interpretation; SJ: paper conceptualisation, editing; FC: paper conceptualisation, editing; ADS: editing.

Competing Interests

We declare no competing interests.

Supplementary Files

This is a list of supplementary files associated with this preprint. Click to download.

- Supplementaryinformation.docx
- TableS1.xlsx
- TableS2.xlsx